

Structure Function of Polymer Nematics: A Monte Carlo Simulation

Randall D. Kamien

*School of Natural Sciences, Institute for Advanced Study, Princeton, NJ 08540 and
Department of Physics and Astronomy, University of Pennsylvania, Philadelphia, PA 19104*

and

Gary S. Grest

*Corporate Research Science Laboratory
Exxon Research and Engineering, Annandale, NJ 08801*

We present a Monte Carlo simulation of a polymer nematic for varying volume fractions, concentrating on the structure function of the sample. We achieve nematic ordering with stiff polymers made of spherical monomers that would otherwise not form a nematic state. Our results are in good qualitative agreement with theoretical and experimental predictions, most notably the bowtie pattern in the static structure function.

PACS: 61.30.G, 61.25.H, 61.20.J

There has been considerable interest recently in a variety of liquids composed of line-like objects aligned on average along a common direction. Flux lines in high-temperature superconductors, strings of electric dipoles in electrorheological fluids and polymer nematics are all systems with this common morphology. Despite the vast literature on nematic liquid crystals, the number of theoretical and experimental studies of polymer nematics is relatively small. Building on work by Meyer [1] and de Gennes [2], statistical mechanical treatments of polymer nematics [3,4] have predicted, in particular, the structure function in the semi-dilute regime. Ao, Wen and Meyer [5] have studied the structure of poly- γ -benzyl-glutamate in the nematic phase by X-ray scattering. However because the experiments cannot reach very small momentum q , due to the forward scattering beam stop, they cannot test many of the main theoretical predictions which are good at these small q values.

We have simulated polymer nematics with the hope of gaining some additional information in the behavior of the polymer nematics. In our simulation nematic order arises *only* due to the polymer stiffness – there is no microscopic, steric nematic interaction. We are particularly interested in the small q region of the static structure function. The resulting equilibrium polymer configurations could be used to compare to actual polymer configurations in nematic solutions of actin [6]. We contrast this study to recent work [7] which studied the phase behavior of 10-mers made of rigid nematogens. In our simulation nematic order arises *only* due to the polymer stiffness – there is no microscopic, steric nematic interaction. Because of the long length scales and slow relaxation times which are inherent in any polymer problem, it is simply not feasible to model in great detail the chemical complexity of any of the experimental polymer nematics such as actin. Fortunately since we are interested in understanding some of the basic properties of polymer nematics, particularly at small q (large distances), it is not necessary to include the chemical detail explicitly. For this reason, we chose to study a coarse grained pearl-necklace model similar to that previously studied for flexible polymer systems [8]. The stiffness of the chain was controlled by adding a three-body bending term which could be tuned to vary the persistence length of our polymer nematic relative to its chain length. Using this model, we are able to test several of the theoretical predictions of [3,4].

We studied an ensemble of M polymer nematics in a periodic rectangular cell. Each monomer of the polymer was modeled by a hard sphere of diameter σ connected to its neighbors along the chain with a fixed bond of length $a = 1.25\sigma$. Results presented here were for $M = 200$ chains of length $N = 50$. Since we are only interested in the static

equilibrium properties of the system and not their dynamics, we used a slithering snake algorithm [9] which is very efficient particularly when the persistence length is large [10]. The algorithm models the reptation motion of a snake by attempting to remove the head (tail) of the chain and placing it at the tail (head) with a random bond angle. We modeled the bond energy as $-\kappa \cos \theta$ where θ is the bond angle, and κ is the bending stiffness measured in units of $k_B T$. If the move violates the excluded volume constraint on the beads, the move is rejected. If not, then the Monte Carlo move is accepted according to the relative energies of the original and new bond angle. The results presented here are from runs made using a force-biased algorithm [11] in which moves are only rejected due to excluded volume. While more moves were accepted compared to a standard Monte Carlo algorithm, the additional complexity did not lead to significant time reduction at high density on either the Silicon Graphics Power Challenge or the IBM Power PC604 (runs were done on both). Since we were interested in rather stiff chains and the rejection rate for the moves was quite high, we quote all times in terms of successful moves [12]. Because of the long runs we concentrated on three areal number densities $\rho_0 \sigma^2 = 0.142$ (areal fraction, $\rho_0 \pi \sigma^2 / 4 = 0.11$), 0.32 (0.25), and 0.569 (0.45). At the highest density the system did not equilibrate and presumably became glassy. We will not report here on the highest density run. We found that the autocorrelation of the end-to-end distance for a single polymer at the bending stiffness we are interested in ($\kappa = 40$) decayed exponentially with a relaxation time of about 1.5×10^5 Monte Carlo moves. Thus we believe that after 1.2×10^8 steps the two lower density runs should have equilibrated. The simulations were started from an initial condition in which all 200 polymers chains were aligned along the z -axis but randomly placed in the xy plane at random heights along the z -axis. At $\rho_0 \sigma^2 = 0.142$, each monomer, on average, moved 15σ laterally, while at $\rho_0 \sigma^2 = 0.32$ each moved 10σ . The chains were placed in a periodic rectangular box with a fixed height $L_z = Na = 62.5\sigma$ in the z -direction and a variable xy area. For the densities we ran at, we found a Maier-Saupe order parameter ($S = [3\langle \cos^2 \theta \rangle - 1]/2$) of 0.049 and 0.849 for $\rho_0 \sigma^2 = 0.142$ and 0.32, respectively, where θ is the angle between the polymer bond and the principal axis with the largest eigenvalue of the bond-moment tensor $T_{ij} = \langle \hat{t}_i \hat{t}_j \rangle$, where \hat{t} is the vector pointing along a bond. Since there was no explicit nematic field added, there is nothing to stop the ordered domain from rotating to a new direction. In the denser run we found that the nematic axis differed from the \hat{z} -axis by approximately 7° . In the most dilute system, since there was no nematic order, the issue was moot. We thus take the z -direction to be the ordering direction for the analysis. In addition, since the starting states had $S = 1$,

the lower average values of the order parameter give us an independent confirmation that the system has equilibrated.

We calibrated the bending energy κ with polymer persistence length for a dilute chain. The persistence length was determined from the bond angle-bond angle correlation length. In Fig. 1, we show the persistence length L_p/a as a function of κ calculated from the first half (solid line) and second half (dashed line) of a 2.4×10^8 step run. Because of the excluded volume interaction, a monomer cannot bend back on its neighbor and the maximum bending angle of a single bond is 133° . This is why the persistence length L_p/a is greater than 1 for $\kappa = 0$. In addition, note that if we were to take the continuum limit, the bending energy would become $\frac{1}{2}\kappa \int (\partial_s \theta)^2$. This simple theory leads to a persistence length $L_p/a = \kappa/k_B T$, in agreement with our calibration when the stiffness is such that self-avoidance is not an issue. In an attempt to match to the experiments of Ao, Wen and Meyer [5] where the polymer persistence length was 80% of the chain length and what can be run in a reasonable amount of time, we concentrate on $\kappa = 40$ for the rest of this paper. This corresponds to a persistence length $L_p/a \approx 39$ and $L_p/[(N-1)a] = 80\%$.

Let us recall the theoretical expectations for the structure function [3,4]

$$S(q_\perp, q_z) = \frac{\langle \delta\rho(q_\perp, q_z) \delta\rho(-q_\perp, -q_z) \rangle}{\rho_0^2}, \quad (1)$$

where q_\perp is the magnitude of $\vec{q}_\perp \equiv (q_x, q_y, 0)$, $\rho = \rho_0 + \delta\rho$ is the local areal number density and ρ_0 is the average mean density. For infinitely long polymers, we expect no scattering along the q_z axis due to the conservation of polymer density along the z -axis. As described by Taratura and Meyer [13], the projection of the polymer tangent into the xy -plane \vec{t} and the areal density ρ satisfy

$$\partial_z \rho + \nabla_\perp \cdot \rho \vec{t} = 0 \quad (2)$$

When $q_\perp = 0$ (2) implies that $\partial_z \rho(q_\perp = 0, z) = 0$. Hence there is no density contrast and there will be no scattering along the $q_\perp = 0$ axis. When the polymers are finite in extent, (2) is modified by adding sources and sinks for polymer heads and tails to the right hand side of the equation. This will lead to some scattering along the q_z axis [4] controlled by the typical polymer length. In addition we expect Bragg-like peaks on the q_\perp axis, corresponding to the incipient columnar crystal being formed by the polymers. Together these two predictions suggest the typical bowtie anisotropic pattern of X-ray scattering.

The average static scattering function $S(\mathbf{q})$ can easily be determined for the simulated system from

$$S(\mathbf{q}) = \frac{1}{NM} \langle |\sum_i \exp(i\mathbf{q} \cdot \mathbf{r}_i)|^2 \rangle. \quad (3)$$

We took the average every 1.2×10^6 moves. Because of the periodic boundary conditions each q_i has to be commensurate with the dimensions of the cell. This means that the smallest nonzero $q_i = 2\pi/L_i$, where i is one of the Cartesian coordinates. Thus as ρ_0 increases at fixed M , the smallest accessible q_i increases, which is one reason we did not study higher density systems. In Fig. 2, we present the results for the two dimensional structure factor $S(q_\perp, q_z)$ for the two densities studied.

Our data agree qualitatively with the first expectation and quantitatively with the second. In addition we calculated the average polymer persistence length for the densities considered. We find $L_P/a = 39$ ($\rho_0\sigma^2 = 0.142$) and 95 (0.32). This is consistent with the increased amount of nematic ordering with increasing density. Note that the value at the lowest density is close to the dilute value of 39.

While the structure function data in the (q_\perp, q_z) plane does not have enough resolution for the fitting of the full two dimensional surface, some information may be gleaned from collapsing the data onto the q_\perp axis. Indeed, the derived function

$$S_2(q_\perp) = \int \frac{dq_z}{2\pi} S(q_\perp, q_z) = \int \frac{dq_z}{2\pi} e^{iq_z z} S(q_\perp, q_z) \Big|_{z=0} = S(q_\perp, z=0) \quad (4)$$

is the structure function of the polymer nematic in any fixed z cross section [4]. Since the numerically determined structure function is only computed for $q_z = -100\pi/L_z \dots 100\pi/L_z$ (where $L_z = Na = 62.5\sigma$ is the height of the box) the sum performed to calculate $S_2(q_\perp)$ will be somewhat smaller than the actual value of $S_2(q_\perp)$. We see the formation of true liquid-like structure in the nematically ordered system and of almost gas-like order in the isotropic system. This is certainly reasonable: the isotropic system is in no sense a directed line-liquid and we should not expect any correlated behavior in a constant z -slice. Note that in the ordered run $S_2(q_\perp)$ has maxima at multiples of $q_0 = 4\pi/(\sqrt{3}a_0)$ where a_0 is the average inter-polymer spacing, indicative of the incipient crystalline order.

In this study we have presented the first Monte Carlo study of a nematic polymer liquid crystal for densities in the semi-dilute regime. We found that for intermediate densities, the static structure function is anisotropic and has the predicted bowtie shape in the (q_\perp, q_z) plane. Using a sum-rule, similar to that relating the structure function at

zero momentum to the bulk compressibility [4] we could extend this work to study the scaling of the bulk modulus over a range of densities. In addition, the sum rule could be checked differently by varying the average polymer length. Polydispersity should not effect the theoretical predictions: this could be checked as well. Finally, a study which varied the persistence length at fixed density would also be enlightening and could be compared to theory.

It is a pleasure to acknowledge stimulating discussions with P. Heiney, J. Käs, F. MacKintosh, R.B. Meyer and D.R. Nelson. The help of T. Tysinger is especially appreciated. RDK would like to thank Exxon Research and Engineering where some of this work was done. RDK was supported in part by the National Science Foundation, through Grant No. PHY92-45317 (IAS), through Grant No. DMR91-22645 and through the National Scalable Cluster Project, Grant No. CDA94-13948 (University of Pennsylvania).

References

- [1] R.B. Meyer, *Polymer Liquid Crystals*, edited by A. Ciferri, W. R. Kringbaum and R. B. Meyer (Academic, New York, 1982) Chapter 6.
- [2] P.G. de Gennes, *Polymer Liquid Crystals*, edited by A. Ciferri, W. R. Kringbaum and R. B. Meyer (Academic, New York, 1982) Chapter 5.
- [3] J. V. Selinger and R. F. Bruinsma, *Phys. Rev. A* **43**, 2910 (1991).
- [4] P. Le Doussal and D. R. Nelson, *Europhys. Lett.* **15**, 161 (1991); R. D. Kamien, P. Le Doussal, and D. R. Nelson, *Phys. Rev. A* **45**, 8727 (1992); *Phys. Rev. E* **48**, 4116 (1993).
- [5] X. Ao, X. Wen and R. B. Meyer, *Physica A* **176**, 63 (1991).
- [6] J. Käs, unpublished.
- [7] M. Dijkstra and D. Frenkel, *Phys. Rev. E* **51**, 5891 (1995).
- [8] A. Baumgärtner, *Ann. Rev. Phys. Chem.* **35** 419 (1984); *Applications of the Monte Carlo Method in Statistical Physics*, edited by K. Binder (Springer, Berlin, 1984).
- [9] F. T. Wall and F. Mandel, *J. Chem. Phys.* **63**, 4592 (1975); F. Mandel, *J. Chem. Phys.* **70**, 3984 (1979).
- [10] We attempted to study this system via a molecular dynamics simulation. We found that equilibration took an unacceptably long time.
- [11] C. Pangali, M. Rao, and B. J. Berne, *Chem. Phys. Lett.* **55**, 413 (1978).
- [12] On the Power PC, a force-biased run of 120 million successful steps took roughly 1000 hours at areal number density $\rho_0\sigma^2 = \frac{\text{number of polymers}}{\text{area in units of } \sigma^2} = 0.32$ (areal fraction, $\rho_0\pi\sigma^2/4 = 0.25$; volume fraction $\phi = 0.13$). On a 143MHz Sun UltraSPARC a force-biased run at $\rho_0\sigma^2 = 0.142$ took roughly 1000 hours. On the Power Challenge (with 75MHz IP21 processors) a non force-biased run of 120 million successful moves took 700 hours for areal number density $\rho_0\sigma^2 = 0.569$ (areal fraction, $\rho_0\pi\sigma^2/4 = 0.45$; volume fraction $\phi = 0.25$). For this case, the acceptance rate is only about 0.3%. This low rate was due to both the rejection rate caused by the bond angle and also the high-densities leading to a small free volume.
- [13] V. G. Taratura and R. B. Meyer, *Liquid Crystals* **2**, 373 (1987).

Figure Captions

- Fig. 1. Single polymer persistence length (in units of the center to center spacing $a = 1.25\sigma$) as a function of the stiffness parameter κ . The solid line shows the persistence lengths measured from a 1.2×10^8 step run, while the dashed line shows the persistence lengths measured in the second half of a 2.4×10^8 step run.
- Fig. 2. Density plots of the polymer structure function in the (q_\perp, q_z) plane. Here $q_0 = 4\pi/\sqrt{3}a_0$, where a_0 is the average inter polymer spacing. Note that there is little scattering along $q_\perp = 0$, in agreement with theoretical arguments. (a) areal number density 0.142 (b) areal number density 0.32.
- Fig. 3. Two-dimensional in-plane structure function for areal number densities 0.142 and 0.32. This is obtained by $S_2(q_\perp) = \int \frac{dq_z}{2\pi} S(q_\perp, q_z)$. The curves are successively shifted along the intensity axis for clarity.

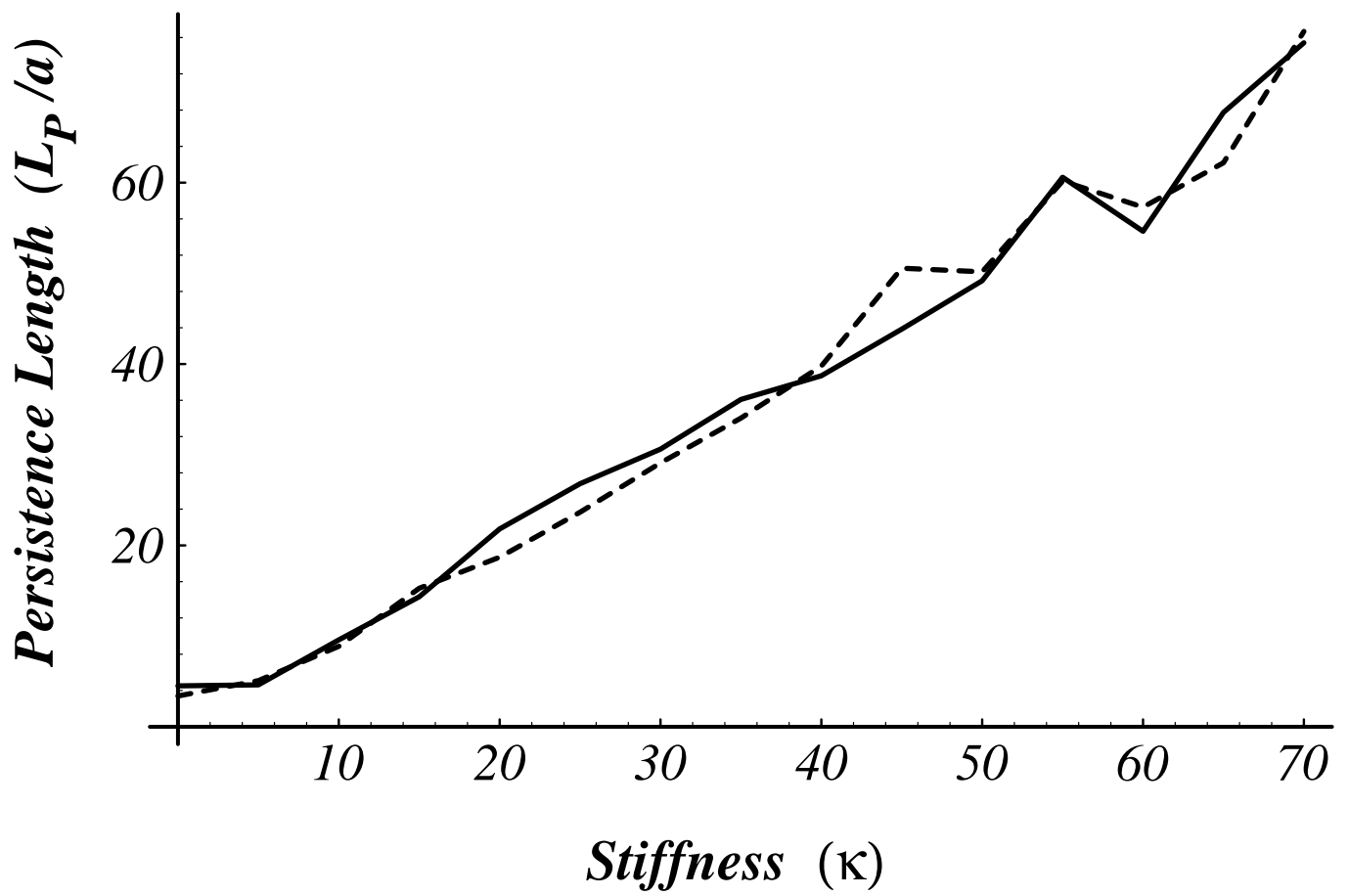


Figure 1

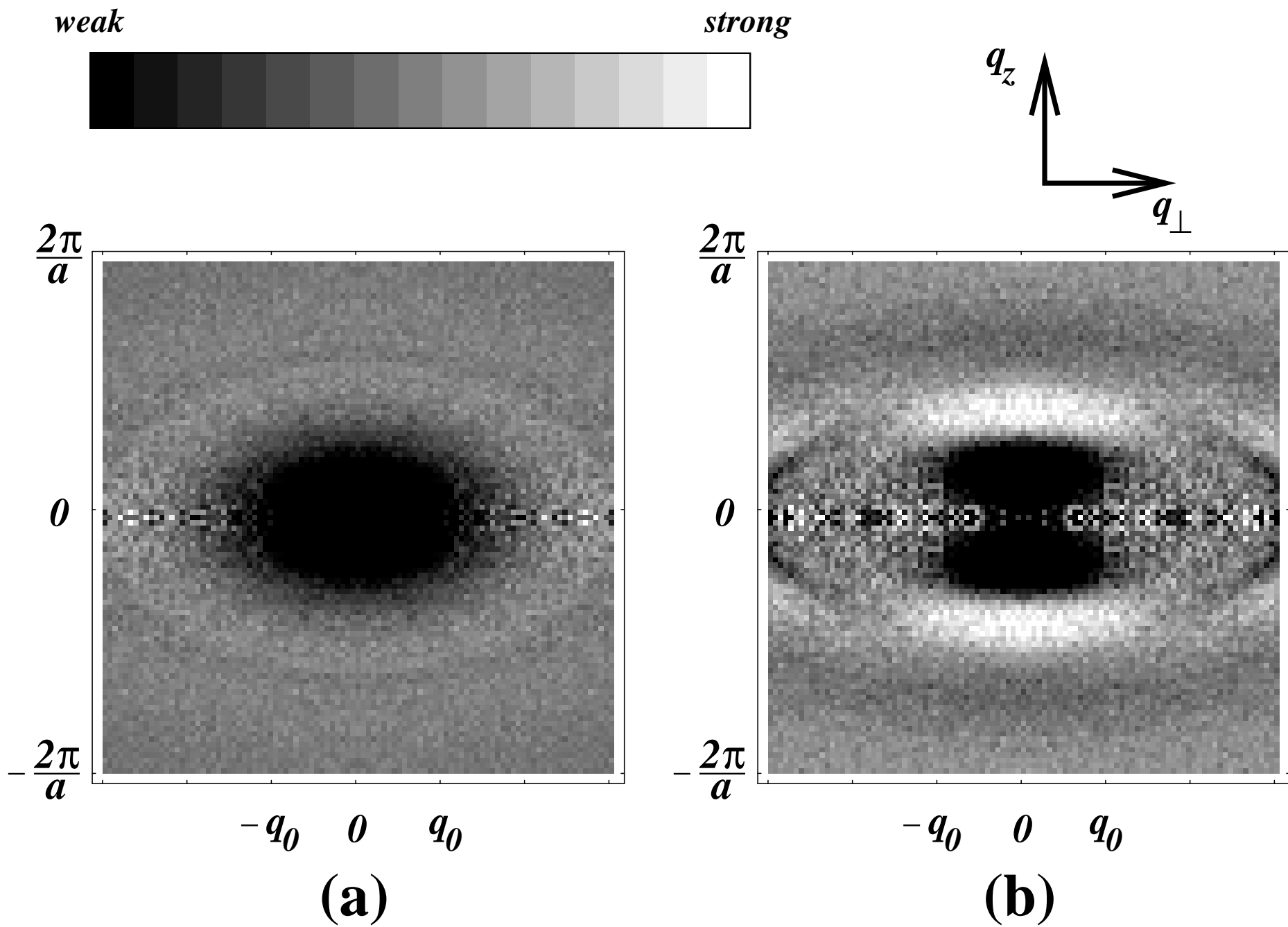


Figure 2

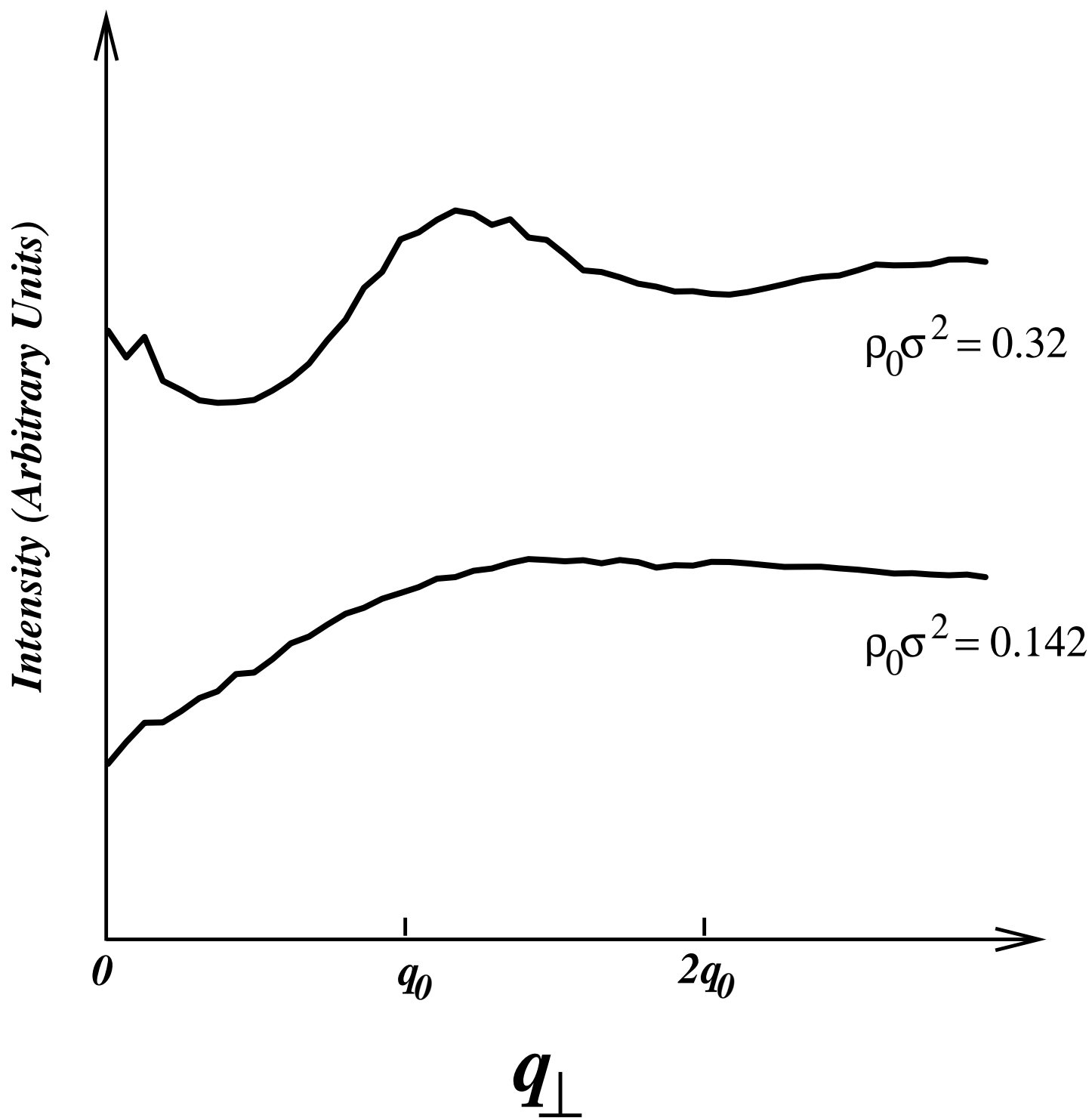


Figure 3